Region specific enhancement of quantum dot emission using interleaved two-dimensional photonic crystals

Gloria G. See,[1] Lu Xu,[2] Matt S. Naughton,[3] Tiantian Tang,[1] Yolanda Bonita,[3] Jake Joo,[5] Peter Trefonas,[5] Kishori Deshpande,[6] Paul J. A. Kenis,[3] Ralph G. Nuzzo,[2] and Brian T. Cunningham[1,4,*]

[1]Department of Electrical and Computer Engineering, University of Illinois at Urbana-Champaign, Micro and Nanotechnology Laboratory, 208 North Wright Street, Urbana, Illinois 61801, USA

[2]Department of Chemistry, University of Illinois at Urbana-Champaign, Frederick Seitz Materials Research Laboratory, 104 South Goodwin Avenue, Urbana, Illinois 61801, USA

[3]Department of Chemical and Biomolecular Engineering, University of Illinois at Urbana-Champaign, Roger Adams Laboratory, 600 South Mathews Avenue, Urbana, Illinois 61801, USA

[4]Department of Bioengineering, University of Illinois at Urbana-Champaign, 1270 Digital Computer Laboratory, MC-278, Urbana, Illinois 61801, USA

[5]Dow Electronic Materials Company, 455 Forest Street, Marlborough, Massachusetts 01752, USA

[6]The Dow Chemical Company, 2301 N. Brazosport Boulevard, Freeport, Texas 77541, USA

*Corresponding author: bcunning@illinois.edu

Received 17 June 2014; revised 12 December 2014; accepted 3 February 2015; posted 9 February 2015 (Doc. ID 214298); published 13 March 2015

The power efficiency, spectral characteristics, and output directionality of light emitting diodes (LEDs) used for lighting and video display may be tailored by integrating nanostructures that interact with photon emitters. In this work, we demonstrate an approach in which visible-wavelength-emitting quantum dots (QDs) are integrated within a polymer-based photonic crystal (PC) and excited by an ultraviolet-emitting LED. The PC design incorporates two interleaved regions, each with distinct periods in orthogonal directions. The structure enables simultaneous resonant coupling of ultraviolet excitation photons to the QDs and visible QD emission at two different wavelengths to efficiently extract photons normal to the PC surface. The combined excitation and extraction enhancements result in a 5.8X increase in the QD output intensity. Further, we demonstrate multiple QD-doped PCs combined on a single surface to optimally couple with distinct populations of QDs, offering a means for blending color output and directionality of multiple wavelengths. Devices are fabricated upon flexible plastic surfaces by a manufacturable replica molding approach.

OCIS codes: (230.5298) Photonic crystals; (230.5590) Quantum-well, -wire and -dot devices; (160.5470) Polymers.

http://dx.doi.org/10.1364/AO.54.002302

1. Introduction

There are a broad range of application-specific needs for lighting and display technologies, given their prevalence in our homes, workplaces, and pockets. Precisely engineered control of the output spectrum

1559-128X/15/092302-07$15.00/0

of lighting products is desired to match the requirements for color temperature and output directionality, while at the same time optimizing power efficiency and manufacturing cost. For video display applications, controlling the blend of primary colors in each pixel is necessary, while the control of pixel output directionality must be tailored for a range of viewing methods that may be either tightly confined (for privacy) or widely dispersed (for wide viewing angle).

As the effects of polarization, wavelength, and directionality within periodic dielectric structures are characterized [1–4], various applications continue to emerge for optical resonators using photonic crystal (PC) structures. By varying the duty cycle, period, and refractive index, the resonant characteristics of a PC can be tuned to interact with wavelengths extending from the ultraviolet [5] to the infrared [6,7]. These properties have been used for a variety of applications including polarizers, filters [8], biosensors [9], optical communication components [10], displays, and lighting [11]. PCs have been incorporated into light emitting diodes (LEDs) in order to increase extraction efficiency [12], and to control the directionality of light output, either normal to the device or into angular sidelobes [13,14].

With an appropriate choice of dielectric materials and dimensions, the resonant modes of a PC can be engineered to occur at specific combinations of angle and wavelength. This allows light of the selected wavelength and incident direction to couple to the PC and excite a highly localized electromagnetic standing wave with an amplitude that is substantially greater than the original illumination source. Enhanced excitation will occur by placing emitters within the region with an increased electric field magnitude at their excitation wavelength. Because the guided modes will couple in and out of the PC under phase matching conditions for specific combinations of wavelength and incident angle, it is possible to collect light at the outcoupling angle more efficiently, and thus providing an enhanced extraction mechanism.

Quantum dots (QDs), semiconductor nanocrystals that down-convert light from a broad band of excitation wavelengths to a very specific emission wavelength [15,16], have been successfully incorporated into PCs with specific resonances designed to couple to the relevant excitation and/or emission wavelengths of the QDs [6,15,17–21]. By introducing two-dimensional variation into the PC structure, through the use of different periods in orthogonal directions, a PC may incorporate multiple resonances at widely varied wavelengths [3] so as to interact simultaneously with the excitation and emission spectra of the integrated QD emitters [17] as a means of enhancing the number of photons generated by each QD, while increasing the efficiency of emitted photons that reach the viewer. In this work, we demonstrate an approach, shown in Fig. 1(a), which incorporates one or more types of QDs into a replica-molded flexible polymer-based PC structure that is excited by a UV backlight LED. The UV excitation source couples to a resonant mode of the PC, which creates an enhanced excitation at the coupling wavelength by increasing the magnitude of the electric field experienced by the QDs in the PC, thus producing greater photon output than would occur without a PC structure. The rectangular lattice of the PC is designed to produce a resonance at the wavelength of QD emission, resulting in photon emission that is efficiently channeled normal to the PC surface. As shown in Fig. 1, we designed and fabricated an interleaved surface in a checkerboard

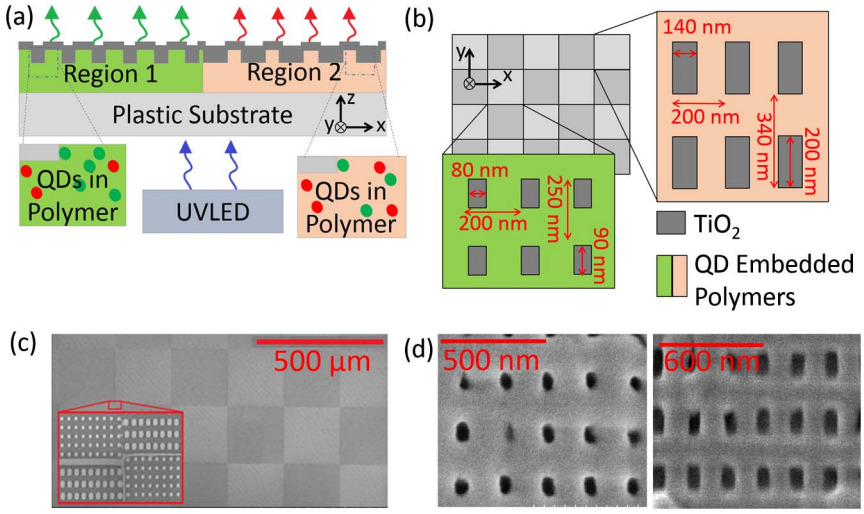

Fig. 1. 2D PC device structure. (a) A cross-sectional schematic of the device structure in which a backlight UV LED source illuminates multiple regions. Each region contains the same QD mix embedded into the polymer layer of the PC grating. However, the two regions have distinct PC structures to enhance and outcouple separate wavelengths of QD emission. (b) A top down schematic of the two interleaved regions of the device with TiO_2 and their respective feature sizes. (c) An SEM of the replica molding master. The inset shows the pillars of the two regions at diagonal corners within the master structure. (d) SEM images of both Region 1 (left) and Region 2 (right) from the device after TiO_2 has been deposited to form the PC.

pattern, containing two PC designs. While both regions are designed to produce resonances for the same UV excitation wavelength, each region is optimized for a different QD emission wavelength. This is a novel device structure that allows multiple types of QDs to experience simultaneous enhancement in a single device structure. Such a structure can enable a customized output spectrum through control of the enhancement wavelengths and the relative surface area of each PC region.

2. Device Structure

The device structure interleaves the regions of two distinct 2D PCs in a checkerboard pattern. Each region consists of rectangular cavities, as shown in Fig. 1(b), with resonances created by the periodic variation in the orthogonal directions on the surface. Each region varies in one direction with dimensions selected to provide enhancement from the same UV excitation source (200 nm period with 40% and 70% duty cycles in Regions 1 and 2, respectively), while the orthogonal directions have larger feature sizes for producing resonances at visible wavelengths. The larger features in Region 1 have a lateral width of 250 nm to produce resonances at $\lambda = 490$ nm, while the features in Region 2 have a lateral width of 340 nm, designed to produce resonances at $\lambda = 590$ nm. For both regions, the structure is formed from a QD-doped polymer with a grating depth of 80 nm that is coated with an 85 nm thin film of TiO_2. While the period of the structure is the main determinant of the resonant wavelength, the resonances can also be tuned via control of the TiO_2 thickness.

The PC structures were designed using rigorous coupled wave analysis (Rsoft, DiffractMod) to predict the resonant wavelengths and electromagnetic field distributions at the resonant wavelengths, by evaluating a unit cell of the PC with periodic boundary conditions in both the x and y directions, as indicated in Fig. 1. Note that, due to the large difference between the refractive index of TiO_2 in the UV ($n = 2.87$) [22] and the visible ($n = 2.61$ at $\lambda = 590$ nm) [22], separate simulations were carried out for unpolarized incident light in two wavelength bands ($350 < \lambda < 450$ nm and $450 < \lambda < 800$ nm) and plotted together for each PC region. The simulation results (Fig. 2) show large dips in the transmission efficiency at the wavelengths for which guided mode resonance occurs. Both regions have resonances in the UV near $\lambda = 370$ nm, and Region 1 has a resonance near $\lambda = 490$ nm, while Region 2 has a resonance near $\lambda = 600$ nm. These visible wavelength resonances are designed to overlap with the emission spectra of QDs incorporated into the PC.

3. Materials and Methods

A silicon wafer was fabricated to serve as a "master" template for the replica molding process, and thus contains a negative surface image of the desired PC grating structure. The master's grating structure

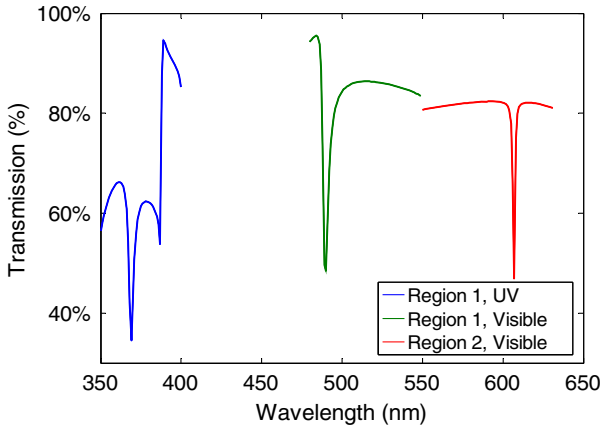

Fig. 2. Computer-simulated transmission spectra of target resonances occurring with an unpolarized source at normal incidence for Regions 1 and 2. Because of the variation in the refractive index values of TiO_2 at different wavelengths, the simulations were run with the appropriate values for each wavelength range.

was fabricated via electron beam lithography on a layer of thermally grown SiO_2 on a Si wafer, upon which reactive ion etching was used to produce 80 nm tall pillars, as shown in Fig. 1(c). The patterned device area was 3 mm × 3 mm. To facilitate the clean removal of the replica from the master, the wafer was cleaned with a piranha solution [3:1(v/v) mixture of sulfuric acid and hydrogen peroxide] for 20 min, rinsed with DI water (MilliQ), and dried with N_2. Next, a vapor-phase deposition of (tridecafluoro-1,1,2,2-tetrahydrooctyl) trichlorosilane (No-Stick, Alfa Aesar) was performed by placing the wafer into an enclosed container with two drops of the No-Stick solution for 1 h.

CdSeS/ZnS alloyed QDs were purchased from Sigma-Aldrich (6 nm, 1 mg/mL in toluene, oleic acid as ligand), or synthesized for this application by coating with oleic acid ligand, then purified twice using precipitation and centrifugation with ethanol and methanol. Lauryl methacrylate (LMA) and ethylene glycol dimethacrylate (EGDMA) (Sigma-Aldrich) were purified to remove the inhibitor with an inhibitor-removal column (Sigma-Aldrich) before their use.

The UV curable polymer, consisting of 182 μL of LMA and 18 μL of EGDMA, was mixed in a flask, and 4 mL of the QD hexane solution and 8 μL oleic acid was added and mixed well, then 20 μL of PLMA monopolymer solution (Scientific Polymer Products, Inc.) was added to increase the viscosity. The remaining solvent was removed using a rotavap at room temperature and 2 μL of initiator (Darocur 1173, Sigma-Aldrich) was added immediately before spin coating. The solution was spin coated onto the master wafer at 600 rpm for 30 s, then immediately polymerized by exposure to a high-intensity UV lamp for 30 min in an argon atmosphere glovebox.

After the film was fully cured, a layer of NOA 61 (Norland Products Inc.) was drop coated over the composite film. An acetate sheet (Optigrafix Acetate)

substrate, selected for low birefringence, was then placed over the master wafer and brought into contact with the uncured NOA drops to form a thin continuous layer between the acetate sheet and the composite thin film. Next, the NOA was cured for 10 min using a UV lamp under ambient conditions. The acetate substrate, along with the NOA layer and composite thin film, was then released from the master wafer with the thin film of QD-PLMA containing the replicated 2D cavity structure. After replica molding, TiO_2 was deposited by sputtering (K. J. Lesker Dual-Gun Sputter System) to the depth required for resonance at the desired wavelength. Deposition times were restricted to keep the substrate temperature from exceeding 40°C, to avoid thermally induced damage to the polymer materials, which sometimes required multiple layers of TiO_2 deposition to reach the correct thickness.

4. Results

The emission properties of the devices were measured using a UV LED (Thor Labs, Ultra Bright Deep Violet LED) centered at $\lambda = 375$ with a 20 nm full width half-maximum as the excitation source. A $350 < \lambda < 390$ nm bandpass filter was used to eliminate any non-UV emission from the LED. The LED output was collimated before illuminating the PC. The device was mounted over a cover with a 3 mm diameter aperture, assuring that only the patterned PC region was excited and measured.

The device under test was mounted to a motorized rotary stage, allowing the incident excitation angle to be varied. The output passed through a UV filter to eliminate any light from the excitation source, then was collected by a collimating lens attached to an optical fiber. The fiber was connected to a spectrometer (USB2000+, Ocean Optics) from which the emission can be measured and observed through the LabView OmniDriver software which also controlled the rotation position of the stage in 0.1 deg steps.

To measure the impact of the extraction angle, the same equipment was used, but instead of mounting the PC sample to a rotation stage and varying the excitation angle, the PC sample position was fixed. The collimator coupled to the optical fiber was instead mounted on the stage and rotated around the PC, allowing extracted light to be collected over a range of angles with respect to the PC surface.

The photonic band diagram of a device was determined using the same experimental setup as that to measure the excitation output, but the UV LED and associated bandpass filter were replaced with a tungsten-halogen lamp coupled to an optical fiber that outputs unpolarized light through a collimator, then the broadband transmission was measured across a range of angles.

In a sample with QDs emitting at a peak wavelength of $\lambda = 505$ nm, the extraction was measured before and after a deposition of 20 nm of TiO_2 to compare the output intensity with and without a photonic crystal structure, as shown in Fig. 3.

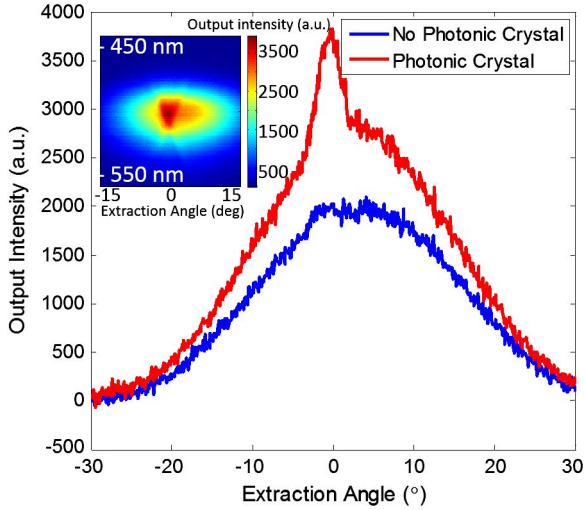

Fig. 3. Impact of angle on QD extraction measured with and without a PC structure present. In the inset, a scan of the output intensities for $\lambda = 450$–550 nm across a range of angles is shown in a device with a 20 nm TiO_2 thin film coating. In the main plot, the angle dependence of the output at $\lambda = 505$ nm is shown. With no PC present, the output emission of the quantum dots is lower. In the structure with the PC, there is a strong angle-dependent enhancement of a factor of $2X$ centered at −2 deg off normal incidence, representing the angle and wavelength combination at which the QD emission is enhanced through resonance with the PC.

A narrow, angle-dependent extraction enhancement is shown, in addition to a broader excitation enhancement. Another sample was fabricated with a homogeneous mixture of QDs, with emissions centered at $\lambda = 490$ nm and $\lambda = 585$ nm. This mix demonstrated the ability of the PC to selectively enhance a subpopulation of embedded QDs. The emission was measured on a QD-doped grating structure without PC resonances by measuring the emission of a structure without TiO_2 [Fig. 4(a)] and after the PC is formed by deposition of a 43 nm TiO_2 thin film. The maximum QD emission increased by 4 times for the 490 nm QDs and 5 times for the 585 nm QDs, shown in Fig. 4(b), but only within the regions in which their emission matched their corresponding PC resonance. To adjust the resonance conditions of the PC for enhancing the emission wavelengths of both types of QDs, an additional 42 nm of TiO_2 was deposited, and that resulted in a total increase of $4.2X$ for the 490 nm QDs and $5.8X$ for the 585 nm QDs [Fig. 4(c)], as the resonance conditions of the PC were redshifted by the thicker TiO_2 layer. After the final TiO_2 deposition, the band structure of the PC was measured using the broadband source, as shown in Fig. 4(d).

Because the device structure has a different period in each orthogonal direction, the transmission efficiency can be measured over the range of angles across θ that vary with the shorter, UV resonant features or the Φ angle with the larger features that couple to visible wavelengths. The difference in the two photonic bands is shown in Fig. 5. In Fig. 5(a), the angle θ is varied, there is an angle-dependent

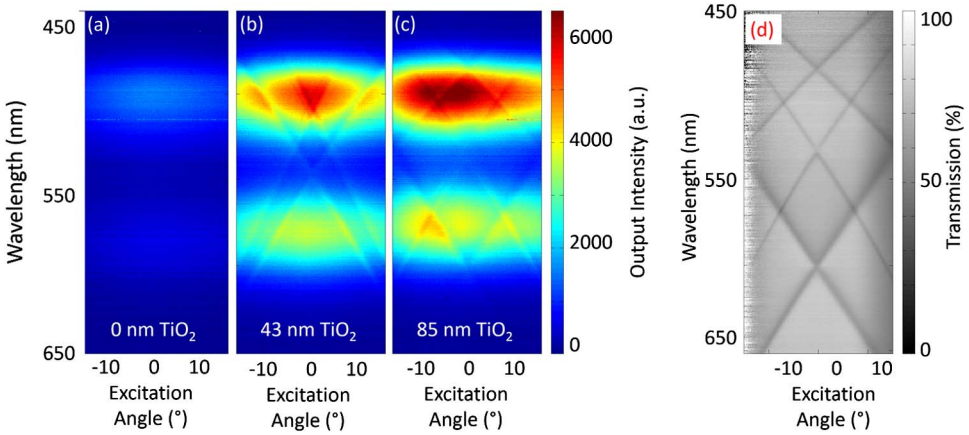

Fig. 4. Comparison of the angle dependence of excitation at different stages of TiO_2 deposition, as the thickness enables tuning of the resonance conditions. (a) Measured output intensity with no PC structure. (b) Measured enhancement from a PC with a 43 nm thick TiO_2 layer. (c) Measured enhancement from a PC with an 85 nm think layer of TiO_2. (d) Transmission spectrum with an 85 nm think layer of TiO_2 confirms the locations of the peak resonance as measured by the varied excitation output intensity in (c).

resonance in the UV, while the resonance in the visible is constant for all wavelengths, regardless of angle. This occurs because there is no angle variation experienced by the features responsible for coupling to those wavelengths. A similar situation occurs in Fig. 5(b) with constant wavelength resonance occurring in the UV wavelengths, while varying the angle Φ experienced by the PC only changes its coupling to the larger PC features and shows angle-dependent variation at wavelengths greater than $\lambda = 450$ nm.

The enhancement of QDs in a region with PC coupling is substantial enough to be easily visible to the naked eye. Figure 6 shows photographs of two dual-region QD-doped PCs with emissions at from $\lambda = 490$ and $\lambda = 590$ nm. The brighter regions are providing both enhanced excitation and extraction for the embedded QDs. The alternate regions have a resonance condition of the PC that is coupling only to the excitation wavelength, and appears darker due to the lack of an extraction enhancement.

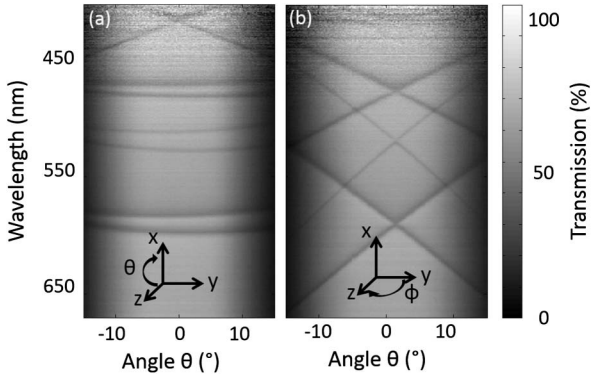

Fig. 5. Resonance conditions for the UV and visible wavelengths occur in orthogonal directions, so in (a), the transmission measured only with angle variation along θ has angle dependence in the coupling to the UV wavelengths. In (b), the Φ variation leads to angle-dependent coupling with the visible wavelengths. The features of the photonic band diagram are less distinct for $\lambda < 450$ nm because the broadband light source emits visible wavelengths $\lambda > 450$ nm.

5. Discussion

The QD excitation measurements for structures with and without a PC structure all showed a slightly asymmetrical output, which corresponded to asymmetrical output intensity from the UV-LED source. This can be seen in Fig. 3, where the peak extraction occurs at −2° from normal incidence. This narrow peak is angle dependent, and shows a factor of 2 increase in output emission with the photonic crystal present, while the broader enhancement across all measured angles is due to the enhanced excitation over the entire PC area. The extraction enhancement occurs only in the PC region, but both regions have resonances at the UV excitation wavelength and so contribute to the enhanced excitation. As shown in Fig. 5, the UV and visible resonances show angle dependence in orthogonal directions, so it is expected that the enhanced excitation shows little angle dependence when varying the extraction angle.

By adjusting the thickness of the TiO_2 layer, the resonance conditions can be easily tuned. As shown

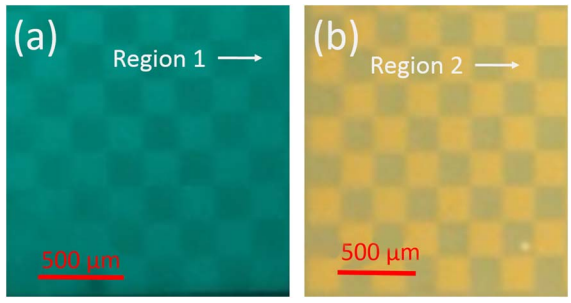

Fig. 6. Photographs of quantum dot enhancement within the checkerboard of PC regions. (a) The QD emission at $\lambda = 490$ nm is brighter in Region 1, where both the excitation and extraction are being enhanced, compared to Region 2, in which only enhanced excitation occurs. (b) A sample with a mix of QDs emitting at $\lambda = 490$ nm and $\lambda = 590$ nm. The yellow QDs in Region 2 dominate the output, because the peak extraction enhancement for $\lambda = 490$ nm in Region 1 is directed away from normal, resulting in reduced intensity when observed from above the PC.

in the varied depositions in Fig. 4(a)–4(c), a thicker layer redshifts the resonance wavelength of the structure. Figure 4(d) shows the photonic band diagram of the structure with the total 85 nm of TiO_2, where the darker bands indicate the wavelength and angle coupling leading to resonance within the PC. These bands correspond to the bands of enhancement seen in Fig. 4(c) within the QD emission.

Devices using the PC structure demonstrated in this work combine excitation and extraction enhancement for an increase of up to 5.8*X* as compared to the QD output produced with no PC structure present. There is an expected difference between the improvements in excitation and extraction, given that the QDs are dispersed through both regions of the PC structure. Therefore, the QDs in every region experience enhancement of the UV excitation wavelength, but the output wavelengths are enhanced only in one region, or half the total device area.

There are also a several mechanisms by which it will be possible to further improve the enhancements offered by this approach. By optimizing the feature sizes for specific colors, the PCs may be designed to better couple to the emission and excitation wavelengths of the desired QDs, increasing the local electric field within the PC, and thus the enhancement experienced in the QD output. This can also be accomplished by coupling QDs to only the TM mode, with higher *Q*-factor resonance conditions. In a 1D PC, the TM mode (which has electric field components in the *x* and *z* directions) can be isolated from the TE mode (with only *y*-directional electric field). However, in a 2D PC, the two polarizations cannot be separated and present as TE- and TM-like modes. These modes are similar to their 1D counterparts, with the TM-like mode occurring at a longer wavelength and having a narrower resonance than the TE-like mode, as shown in the band diagram in Fig. 4.

In addition, the lattice structure in the PC has a dramatic effect on the possible enhancement, as shown in [9,20], where square and hexagonal arrangements of circular cavities demonstrated enhancement factors of 100–200*X*. Specifically placing the QDs only in the PC pixel region where they would experience both excitation and extraction would decrease the quantities of QDs required and also extract light more effectively. With these improvements, it is likely that the PC enhancement would be at least comparable to the 8*X* enhancement reported in [17].

Future devices may be designed to utilize a non-UV excitation source simply by adjusting the design parameters to couple to a different wavelength. Pixel patterning can also create regions with no PC structure at all, allowing only the excitation source light to pass through, thus increasing the flexibility of color mixing options for lighting.

The use of nanoreplica molding for fabrication makes it possible to scale up to large area fabrication on flexible substrates. With appropriate materials, large area, flexible displays and light sources can be constructed to use pixelated PC enhancement. The use of PCs in lighting and displays gives the advantage of angle steering possible with PC enhancement to broaden or narrow the output angles and control the directivity of light output in both lighting and displays. Polarization control is also possible with a PC, and could eliminate the 50% loss of backlight power by providing an initially polarized output in display technology.

The technological opportunities afforded by PCs combined with the levels of enhancement possible using QD-embedded PC devices may be a key enabler for the affordable incorporation of QDs into novel lighting and display applications. The enhancements require lower concentrations of QDs and could advance the color purity and performance of QD-based light sources toward consumer applications.

6. Conclusions

The devices in this work demonstrate the incorporation of QDs into a replica molded 2D PC. The PC has distinct periods in orthogonal axes, allowing one direction of the structure to resonantly couple the UV LED excitation source to the embedded QDs. The orthogonal direction resonantly couples to the QD emission in the visible spectrum, enhancing the extraction of photons normal to the device surface. These structures have demonstrated combined excitation and extraction enhancements up to 5.8*X* output intensity, using an approach that interleaves PC regions and enables design-selectable resonant properties, allowing different types of QDs to be embedded into the device and experiencing simultaneous enhancement from the same excitation source, but different extracted wavelengths. The resulting pixelated surface on a flexible substrate enables blending of the color and directional output of multiple QD emission wavelengths for potential lighting or display applications.

The authors are grateful for the support of Dow Chemical Company under Research Agreement #226772AC.

References

1. A. Hessel and A. A. Oliner, "A new theory of Wood's anomalies on optical gratings," Appl. Opt. **4**, 1275–1297 (1965).
2. Y. Ding and R. Magnusson, "Band gaps and leaky-wave effects in resonant photonic-crystal waveguides," Opt. Express **15**, 680–694 (2007).
3. Y. Ding and R. Magnusson, "Resonant leaky-mode spectral-band engineering and device applications," Opt. Express **12**, 5661–5674 (2004).
4. J. D. Joannopoulos, S. G. Johnson, J. N. Winn, and R. D. Meade, *Photonic Crystals, Molding the Flow of Light* (Princeton University, 2008).
5. N. Ganesh and B. T. Cunningham, "Photonic-crystal near-ultraviolet reflectance filters fabricated by nanoreplica molding," Appl. Phys. Lett. **88**, 071110 (2006).
6. M. Rippa, R. Capasso, P. Mormile, S. De Nicola, M. Zanella, L. Manna, G. Nenna, and L. Petti, "Bragg extraction of light in 2D photonic Thue–Morse quasicrystals patterned in active CdSe/CdS nanorod-polymer nanocomposites," Nanoscale **5**, 331–336 (2013).

7. A. K. Kodali, M. Schulmerich, J. Ip, G. Yen, B. T. Cunningham, and R. Bhargava, "Narrowband midinfrared reflectance filters using guided mode resonance," Anal. Chem. **82**, 5697–5706 (2010).
8. R. Magnusson and S. Wang, "New principle for optical filters," Appl. Phys. Lett. **61**, 1022–1024 (1992).
9. N. Ganesh, I. D. Block, P. C. Mathias, W. Zhang, E. Chow, V. Malyarchuk, and B. T. Cunningham, "Leaky-mode assisted fluorescence extraction application to fluorescence enhancement biosensors," Opt. Express **16**, 21626–21640 (2008).
10. J. Herrnsdorf, B. Guilhabert, J. J. D. McKendry, Z. Gong, D. Massoubre, S. Zhang, S. Watson, A. E. Kelly, E. Gu, N. Laurand, and M. D. Dawson, "Hybrid organic/GaN photonic crystal light-emitting diode," Appl. Phys. Lett. **101**, 141122 (2012).
11. K.-S. Cho, E. K. Lee, W.-J. Joo, E. Jang, T.-H. Kim, S. J. Lee, S.-J. Kwon, J. Y. Han, B.-K. Kim, B. L. Choi, and J. M. Kim, "High-performance crosslinked colloidal quantum-dot light-emitting diodes," Nat. Photonics **3**, 341–345 (2009).
12. C. Wiesmann, K. Bergenek, N. Linder, and U. T. Schwarz, "Photonic crystal LEDs—designing light extraction," Laser Photon. Rev. **3**, 262–286 (2009).
13. K. McGroddy, A. David, E. Matioli, M. Iza, S. Nakamura, S. DenBaars, J. S. Speck, C. Weisbuch, and E. L. Hu, "Directional emission control and increased light extraction in GaN photonic crystal light emitting diodes," Appl. Phys. Lett. **93**, 103502 (2008).
14. A. Z. Khokhar, K. Parsons, G. Hubbard, I. M. Watson, F. Rahman, D. S. Macintyre, C. Xiong, D. Massoubre, Z. Gong, E. Gu, N. P. Johnson, R. M. De La Rue, M. D. Dawson, S. J. Abbott, M. D. B. Charlton, and M. Tillin, "Emission characteristics of photonic crystal light-emitting diodes," Appl. Opt. **50**, 3233–3239 (2011).
15. D. Englund, D. Fattal, E. Waks, G. Solomon, B. Zhang, T. Nakaoka, Y. Arakawa, Y. Yamamoto, and J. Vučković, "Controlling the spontaneous emission rate of single quantum dots in a two-dimensional photonic crystal," Phys. Rev. Lett. **95**, 013904 (2005).
16. J. N. David, "Electronic structure in semiconductor nanocrystals," in *Nanocrystal Quantum Dots*, 2nd ed. (CRC Press, 2010), pp. 63–96.
17. F. Yang and B. T. Cunningham, "Enhanced quantum dot optical down-conversion using asymmetric 2D photonic crystals," Opt. Express **19**, 3908–3918 (2011).
18. M. Barth, A. Gruber, and F. Cichos, "Spectral and angular redistribution of photoluminescence near a photonic stop band," Phys. Rev. B **72**, 085129 (2005).
19. F. S. Diana, A. David, I. Meinel, R. Sharma, C. Weisbuch, S. Nakamura, and P. M. Petroff, "Photonic crystal-assisted light extraction from a colloidal quantum dot/GaN hybrid structure," Nano Lett. **6**, 1116–1120 (2006).
20. N. Ganesh, W. Zhang, P. C. Mathias, E. Chow, J. A. Soares, V. Malyarchuk, A. D. Smith, and B. T. Cunningham, "Enhanced fluorescence emission from quantum dots on a photonic crystal surface," Nat. Nanotechnol. **2**, 515–520 (2007).
21. L. Petti, M. Rippa, J. Zhou, L. Manna, M. Zanella, and P. Mormile, "Novel hybrid organic/inorganic 2D quasiperiodic PC: from diffraction pattern to vertical light extraction," Nanoscale Res. Lett. **6**, 371 (2011).
22. J. R. Devore, "Refractive indices of rutile and sphalerite," J. Opt. Soc. Am. **41**, 416–417 (1951).